Sustainable Chemistry and Pharmacy 48 (2025) 102260

Contents lists available at ScienceDirect

Sustainable Chemistry and Pharmacy

journal homepage: www.elsevier.com/locate/scp

The quest for the new CaLB: Potential of three thermostable polyester hydrolases for esterification reactions

Francesco Papatola [a], Filippo Fabbri [b], Virender Kumar [c], Chiara Siracusa [b,d], Felice Quartinello [b,d], Doris Ribitsch [b], Cristiano Varrone [c], Georg M. Guebitz [b,d], Alessandro Pellis [a,*]

[a] Università di Genova, Dipartimento di Chimica e Chimica Industriale, Via Dodecaneso 31, 16146, Genova, Italy
[b] Institute of Environmental Biotechnology, Department of Agrobiotechnology, IFA-Tulln, BOKU University, Konrad Lorenz Strasse 20, Tulln an der Donau, 3430, Austria
[c] Department of Chemistry and Bioscience, Aalborg University, 9220, Aalborg, Denmark
[d] Austrian Centre of Industrial Biotechnology, Konrad Lorenz Strasse 20, Tulln an der Donau, 3430, Austria

ARTICLE INFO

Keywords:
α,β-hydrolases
Enzyme immobilization
Design of experiment (DoE)
Biocatalzyed synthetic reactions
Enzymatic polycondensation

ABSTRACT

The potential of three thermophilic enzymes from the α,β-hydrolases superfamily, that have recently been described for polyester hydrolysis, was investigated for polyester synthesis, esterification and transesterification reactions. The hydrolases (LCC, leaf-branch compost cutinase; its variant LCC^{ICCG}, Thb from *Thermoanaerobacterales* bacterium) were recombinantly expressed, purified and immobilized onto polypropylene beads. A design of experiments (DoE) assisted study was performed to investigate their synthetic potential to produce short flavor esters by analyzing their thermostability and selectivity towards alcohols and acids with different chain lengths. The factors considered in the DoE (i.e., temperature, alcohol chain length, acid chain length and reaction time) were optimized using MODDE® software to generate a predictive model defining the optimal synthetic conditions for the three enzymes. In each experiment, the monitored response was the acid conversion rate, quantified with GC-FID analysis. For synthesis, the temperature optima of LCC, LCC^{ICCG} and Thb were 60 °C, 55 °C, and 80 °C, respectively, corresponding to the maximum percentage of monomers conversion for long-chain alcohols and acids as substrates. Polymerization of dimethyl adipate and 1,8-octanediol as building blocks was carried out to confirm the applicability of the obtained model for the synthesis of larger macromolecules via polycondensation reactions. The proposed approach highlights the innovative application of these novel thermophilic enzymes, traditionally associated with hydrolytic functions, as effective biocatalysts in synthetic processes, enabling the production of a well-known class of polyesters through an alternative and sustainable enzymatic route. Conversion of monomers, as determined by nuclear magnetic resonance (NMR) analysis, was ~90 % for all enzymes while the average molecular weights (M_n) of the polyesters, analyzed by gel permeation chromatography, were between 3600 Da, for LCC and its variant LCC^{ICCG}, and 3800 Da for Thb.

* Corresponding author.
E-mail address: alessandro.pellis@unige.it (A. Pellis).

https://doi.org/10.1016/j.scp.2025.102260
Received 2 September 2025; Received in revised form 24 October 2025; Accepted 4 November 2025
Available online 5 November 2025

1. Introduction

Scientific advances in the field of biocatalysis have led to the development of promising enzymes thus opening extraordinary opportunities not only in the conventional sector of food and detergents but also in green processes having deep impact on health (e.g., pharmaceuticals and cosmetics), environmental protection (e.g., agrochemicals) as well as for the production of fine-chemicals and polymers(Illanes et al., 2012; Ran et al., 2008). Nowadays, enzymes are extensively employed for textile processing and in many other applications like polymer decomposition. For example, certain hydrolases can hydrolyze polyesters such as poly(ethylene terephthalate) (PET)(Arnal et al., 2023; Han et al., 2017) allowing selective recovery of valuable building blocks even from blends and mixed wastes. On the other hand, under specific conditions, enzymes are able to catalyze the reversed reaction to synthetize aliphatic and aromatic-aliphatic polyesters or oligomers with side chains functionalities. In response to the growing demand for bio-based and biodegradable polymers, aligned with the principles of the "European Green Deal"(Tao and Kazlauskas, 2011), enzymes have emerged as a promising and sustainable alternative to the traditional chemical synthetic pathways offering a viable solution to the ongoing challenge of reconciling mild reaction conditions with high catalytic efficiency and selectivity(Pellis et al., 2016a). Unlike traditional chemical processes, enzymes operate under relatively low temperatures (typically <100 °C)(Pellis et al., 2018) and ensure environmentally friendly processes avoiding the use of toxic metal catalysts such as tin and titanium, which are commonly employed in conventional polycondensation reactions(Williams, 2007). In this context, biocatalysis is increasingly acknowledged as a powerful strategy in modern chemical manufacturing for the production of bio-based and biodegradable polyesters, offering an environmentally friendly alternative that allow the design of functional polymers which are difficult to achieve via traditional metal-catalyzed reactions (Guarneri et al., 2019).

Despite their significant catalytic potential, a broader use of enzymes in this field remains constrained by limitations such as inadequate long-term stability, challenging recovery and the inability to reuse the costly enzymes. These challenges may be addressed by employing enzyme immobilization strategies which facilitate efficient separation of the biocatalyst from the reaction mixture, thereby simplifying its recovery and re-use, while also enhancing key enzymatic properties such as activity, stability and substrate specificity(Hanefeld et al., 2009; Sheldon, 2007; Sheldon and van Pelt, 2013).

Nowadays, mainly lipases are used for synthetic reactions, with *Candida antarctica* lipase B (CaLB) being the most commonly employed enzyme for the synthesis of polyesters and flavor esters. This prominence could be attributed to its commercial availability in both free and immobilized form(Pellis et al., 2016b), as well as its remarkable properties, including high catalytic efficiency and excellent selectivity. In particular, CaLB, in its immobilized form on acrylic resin (commercially available as Novozym 435, N435), has emerged as the most intensively employed biocatalyst in synthetic applications(Mahapatro et al., 2003). Pellis et al. reported the CaLB selectivity pattern in which immobilized enzyme (N435) showed its preference towards long-chain diols and diesters instead of short-chain compounds in polycondensation reactions obtaining the best combination using dimethyl adipate and 1,8-octanediol at 85 °C with high M_n products (7000 Da)(Pellis et al., 2018). Moreover, other enzymes classified within the α,β-hydrolases superfamily have been extensively investigated as biocatalysts for polyesters synthesis. Among these, the commercial *Humicola insolens cutinase* (HiC)(Kobayashi and Makino, 2009; Hunsen et al., 2007) or the more recently reported *Thermobifida cellulosilytica cutinase* 1 (Thc_Cut1)(Pellis et al., 2017a, 2017b) have demonstrated promising catalytic performance. In particular, Feder and Gross demonstrated that HiC, when immobilized on Amberzyme oxirane resin, exhibits a high selectivity towards long-chain diols and diacids. Their study revealed an enzyme preference for substrate like dimethyl sebacate and 1,8-octanediol at 70 °C, leading to the formation of polyesters reaching M_{ns} of 6600 Da(Feder and Gross, 2010). Conversely, Thc_Cut1, immobilized on different carriers (such as opal, coral, and amber beads), preferred short chain diol, independent of the diester chain length (C6, C8, or C10), in reactions performed at 50 °C. Differently from reactions employing this kind of supports, where polyesters with a limited molecular weight of 900 Da were produced(Pellis et al., 2017b), products with higher M_w (~1900 Da) were achieved when the same enzyme was covalently bound on epoxy resins(Pellis et al., 2016a).

Furthermore, in addition to what was previously proven in the literature on different CaLB/HiC/Thc_Cut1 immobilized preparations, Fabbri et al. developed a full-factorial design of experiments to investigate the thermostability and selectivity of these three commercial hydrolytic enzymes (i.e., CaLB, HiC and Thc_Cut1) immobilized onto polypropylene beads confirming the data previously reported in the literature(Fabbri et al., 2021).

Esterases, lipases and cutinases primarily split ester bonds in different small and larger molecules, but under low water or organic solvent conditions due to their reversible catalytic mechanism and α/β-hydrolase fold, they can also catalyze esterification and transesterification. This study aims to identify novel thermophilic enzymes suitably for synthesis belonging to the α,β-hydrolases superfamily which have been described to hydrolyze polyesters. For the first time, in this work, three efficient PET hydrolases, namely leaf-branch compost cutinase LCC(Sulaiman et al., 2012; Kumar et al., 2024), its mutant form ICCG (LCC^{ICCG}) engineered to improve the thermostability and activity of LCC in depolymerization and recycling activities(Tournier et al., 2020; Li et al., 2023), and Thb (from *Thermoanaerobacterales bacterium* with high homology to PHL7)(Richter et al., 2023; Sonnendecker et al., 2022; Siracusa et al., 2025) were tested in synthesis reactions. The three hydrolases were adsorbed onto polypropylene beads to assess their catalytic efficiency in the synthesis of short-esters while evaluating their thermostability and selectivity towards alcohols and acids of varying chain length. A design of experiments (DoE) assisted study was implemented and the results on flavor esters helped determining the Temperature optimum (T_{opt}) of the three enzymes which were subsequently applied to enzymatic polycondensations using bio-based monomers (i.e., dimethyl adipate and 1,8-octanediol) as building blocks for polyester synthesis, aiming to confirm the applicability of the obtained models also on larger macromolecules.

2. Experimental

2.1. Materials and methods

Polypropylene beads (Accurell MP1000 surface area of 55,985 m^2g^{-1}, particle density of 1.993 cm^{-3}, and particle diameter of <1500 μm) were obtained from 3 M Deutschland GmbH (Wuppertal, Germany). Dimethyl adipate (DMA, >99 %), 1,8-octanediol (ODO, >98 %), butyric acid (>99 %), 1-butanol (>99 %), 1-octanol (>99 %), Octanoic acid (>98 %), 1-dodecanol (>99 %), lauric acid (>99 %), 2-methyl 2-butanol (>99 %), 4-nitrophenol (>99 %), *para*-nitrophenyl butyrate (*p*-NPB), K_2HPO_4 (>98 %) and KH_2PO_4 (>98 %) were purchased from Sigma-Aldrich. Chloroform ($CHCl_3$ for GC analysis, >99.8 %), Chloroform-d ($CDCl_3$ for ^1H NMR) and tetrahydrofuran (THF for GPC, >99 %) was purchased from VWR Chemicals (Wien, Austria). The amino acid sequences corresponding to LCC, LCC^{ICCG} and Thb were obtained from the Protein Data Bank (PDB) database and subsequently codon-optimized for the expression in *Escherichia coli* BL21-(DE3). Lysogeny Broth (LB), kanamycin and isopropyl-β-D-thiogalactoside (IPTG) were sourced from Sigma-Aldrich (Germany). Escherichia coli BL21-Gold (DE3) electrocompetent cells were obtained from Agilent.

2.2. Expression and purification of enzymes

The three enzymes (i.e., Leaf-branch compost cutinase LCC; its mutated form LCC^{ICCG}; and the hydrolase from *Thermoanaerobacterales* (Thb), were expressed in the electrocompetent *E. coli* strain BL21-(DE3) using pET26b(+) vector. LCC and LCC^{ICCCG} were produced and purified as previously described by Kumar et al., 2024, 2025, while Thb was produced and purified following the method reported by Siracusa et al. (2025). Purification efficiency was assessed through an SDS-PAGE analysis. Aliquots from load, flow-through, and eluted fractions were mixed in Laemmli buffer with 2-mercaptoethanol and then loaded onto precast Mini-PROTEAN TGX Stain-Free gels (Bio-Rad). Electrophoresis was left to run at 150 V for 30 min and an already known molecular weight protein marker IV (Peqlab, Germany) was used as reference. As visible from Fig. S1, SDS-PAGE analysis revealed a molecular weight of 30 kDa for both LCC and LCC^{ICCG}, while the molecular weight of Thb was 35 kDa.

2.3. p-NPB based Esterase Activity Assay

The esterase activity of the three enzymes was determined based on hydrolysis of *para*-nitrophenyl butyrate (*p*-NPB). The catalytic activity was calculated by evaluating the increase in absorbance at 405 nm, resulting from the release of *p*-nitrophenol (ε 405 nm). 200 μL of substrate solution were mixed with 20 μL of the enzyme, previously diluted in 0.1 M K_2HPO_4/KH_2PO_4 buffer at pH 8 (referred as KPO). Measurements were performed every 18 s over a 5-min period using a Tecan Plate Reader (Tecan, Grödig, Austria) and 96-well microtiter plates (Greiner 96 Flat Bottom Transparent Polystyrene). The samples were analyzed in triplicates and a series of blanks (i.e., buffer without enzyme) were included in each activity cycle. The enzymatic activity of LCC, LCC^{ICCG} and Thb was expressed in units (U), where one U corresponds to the amount of enzyme that catalyzes conversion of 1 μmol per minute, and resulted to be 68.4 (σ = 1.2) U/mg, 57.2 (σ = 0.7) U/mg and 49.2 (σ = 0.8) U/mg, respectively. A qualitative *p*-NPB based Esterase Activity Assay was also performed to obtain visual detection evidence of enzymatic activity post-immobilization.

2.4. Determination of protein concentration

Protein concentrations of the three enzymes dissolved in KPO was determined using the Bio-Rad solution (Coomassie brilliant blue G-250 dye) diluted 1:5 in milliQ water. Different solutions of BSA (Bovine Serum Albumin, 2 mg/mL, Sigma-Aldrich) were used as standard protein to obtain a calibration curve (Fig. S2), from which it was possible to determine protein concentration of LCC, LCC^{ICCG} and Thb (0.5 mg/mL, 0.96 mg/mL and 0.72 mg/mL respectively). BSA standard was serially diluted in KPO buffer to get the following concentrations: 0.0625, 0.1, 0.125, 0.2, 0.25, 0,4, 0.5, 1 and 2 mg/mL. Absorbance was recorded at 595 nm (resulted from the dye's interaction with primarily basic and aromatic aa residue of the protein, ε 595 nm) with a Tecan Plate Reader (Tecan, Grödig, Austria) using a 96-well microtiter plate (Greiner 96 Flat Bottom Transparent Polystyrene). 10 μL of each sample (both BSA and enzyme solutions) were put in the wells and 200 μL of 1:5 BioRad solution were added (in triplicate), incubating the mixture for 5 min at RT before analysis. A blank was also included using the KPO buffer.

2.5. Enzyme immobilization procedure

In a 50-mL Falcon™ tube, 1.0 g of polypropylene beads were accurately weighed and washed three times with 20 mL of acetone at 400 mbar for 5 min to remove the air and facilitate the enzyme loading in the bead's cavities. Subsequently, the beads were first rinsed with 20 mL of deionized H_2O and then twice with 20 mL of the immobilization buffer (KPO buffer pH 8). All washing procedures were performed using a blood rotator (SB3 model from VWR), set at constant speed of 30 rpm. Afterwards, 40 mL of enzyme solutions (0.25 mg/mL corresponding to 1 % w/w enzyme/beads) were added to the beads. The mixture was incubated for 24 h on the blood rotator (RT at 30 rpm). Aliquots were collected over time (0, 1, 2, 4, 8, 24 h) to monitor the progression of immobilization by analyzing the residual enzyme activity (via *p*-NPB based Esterase Activity Assay) and residual protein concentration (via Bradford-based Bio-Rad Protein Assay) in the supernatant. After 24 h, the beads were recovered by filtration using a paper filter, washed 3 times with KPO buffer and air-dried for 3 days at RT.

2.6. Three-level full factorial design of experiment (DoE)

A 3-level full factorial experimental design was developed using MODDE® Pro 13 Software (Sartorius) to investigate thermostability and substrate selectivity of LCC, LCC^{ICCG} and Thb. The DoE was planned to evaluate all the possible interactions among four selected independent variables studied at 3 levels (i.e., temperature = 50 °C, 70 °C, and 90 °C; alcohol chain length = C4, C8, and C12; acid chain length = C4, C8 and C12; and reaction time = 2, 4, and 6 h) aiming to assess the combined effect of each parameter on the response variable. The experiments were carried out in a randomized order for a total number of 81 reactions for each enzyme (i.e., 4 factors are studied at 3 levels by performing 3^4 experiments). Additionally, a central point, defined by combination of all independent variables taken at their intermediate levels (specifically: temperature = 70 °C; alcohol = C8; acid = C8; time point = 4 h), was added in the experimental design. The response variable assessed for each condition was the acid conversion rate, determined by Gas Chromatography (GC) analysis.

2.7. Enzymatic esterification reactions

The reactions for short-esters synthesis were conducted by mixing, in a 50 mL reaction tube, equimolar amounts (6.0 mmol) of dicarboxylic acid and alcohol with an amount of immobilized enzyme (1 % w/w enzyme/beads), corresponding to 2.5 % in weight referred to as the total amount of monomers (2.5 % w/w enzyme/total monomers weight). To determine the T_{opt} of LCC, LCC^{ICCG} and Thb for the reactions, enzymatic esterification reactions were performed at three different temperatures (50 °C, 70 °C and 90 °C) using the multipoint reactor Carousel 12 plus reaction station purchased (Radleys, Saffron Walden, UK). Every 2 h (2, 4, and 6 h), 10 μL aliquots were collected from each reaction mixture. Each aliquot was subsequently diluted in 10 mL of $CHCl_3$ and spiked with 10 μL of toluene as an internal standard. In parallel, a blank of each performed reaction was carried out in the absence of the biocatalyst. All the aliquots were then analyzed through gas chromatography (GC) analysis. In accordance with the established chemical mechanism of CaLB(Kobayashi, 2010), the three enzymes operate through a ping-pong bi-bi mechanism, a double displacement reaction typical of multi-substrate enzymatic systems. In this process, the enzymes first reacts with a substrate to generate the first product and a transiently modified enzyme form; this intermediate then engages a second substrate, releasing a second product and regenerating the native enzyme(Loos, 2022). The alternating sequence of substrate binding and product formation reflects the characteristic "ping--pong" dynamics of the mechanism.

2.8. Gas chromatography (GC) analysis

The samples obtained from the enzymatic esterification reaction, and subsequently prepared as described in section 2.7, were diluted 1:4 by mixing 250 μL of the reaction mixture with 750 μL of $CHCl_3$ in 1.5-mL HPLC vials. GC analysis was performed over a 45-min run up to 250 °C, using $CHCl_3$ as the needle washing solvent. The GC analysis was conducted using an Agilent Technologies 6890 N Network GC system (Agilent Technologies, Santa Clara, CA, USA) equipped with a J&W DB-FFAP column (Part No.122-3232; nominal dimension of 30.0 m × 250 μm x 0,25 μm; 250 °C of maximum operating temperature). The Injector (HO 6890 series) was operated with hydrogen as the carrier gas at a flow rate of 40 mL/min, an airflow rate of 450 mL/min, and nitrogen makeup flow equal to 20 mL/min.

2.9. Enzymatic synthesis of polyesters

Enzymatic polycondensation of dimethyl adipate and 1,8-octanediol was performed in solvent-less condition as previously reported by Pellis et al. (2015). Equimolar amounts of the two monomers (3 mmol) were mixed in 25-mL round-bottom flask with an amount of immobilized enzyme (1 % w/w enzyme/beads), corresponding to 10 % in weight referred to as the total amount of monomers (10 % w/w enzyme/total monomers weight). Once the enzyme was added, the reaction was carried out for 6 h under ambient pressure to prevent the loss of volatile monomers, at the corresponding $T_{opt.}$, previously determined from esterification reactions for all the three enzymes. Afterwards, 25 mL round-bottom flask were connected to a Schlenk line linked to a BÜCHI vacuum pump in order to reduce the pressure at 15 mbar. This reduced pressure was maintained for 18 h, while maintaining the corresponding $T_{opt.}$, both to remove the by-product, MeOH, that was formed during the reaction, and to facilitate the elongation of the polyester. After a total reaction time of 24 h, the reaction mixture was processed by dissolving the resulting products in Me-THF. The biocatalyst, immobilized on polypropylene beads, was subsequently separated via filtration through a cotton filter. After solvent removal, the resulting polyesters were subjected to characterization without any additional purification steps.

2.10. Polyester characterization: proton nuclear magnetic resonance (^1H NMR) and gel permeation chromatography (GPC)

The ^1H NMR spectra were acquired using a JEOL ECZ-400R/S3 NMR spectrometer equipped with a 5 mm broadband Royal HFX probe. The operating frequency was 400 MHz using deuterated chloroform ($CDCl_3$) as the solvent. For each measurement, approximately 10 mg of polyester was dissolved in 700 μL of $CDCl_3$. Gel permeation chromatography (GPC) analyses were performed using sample solutions prepared at concentration of 2 mg/mL. Analytical-grade THF, stabilized with BHT, was used consistently both as solvent for sample preparation and mobile phase during chromatographic separation. The GPC system operated under the following conditions: an injection volume of 100 μL, a flow rate of 1.00 mL/min and an elution time of 18 min. The column temperature was maintained at 35 °C with an isocratic Pump pressure of 39 bar. Detection was performed using a refractive index detector set at 35 °C

and separation was achieved using an Agilent GPC/SEC Plgel 5 μm MIXED-C column (300 × 7.5 mm), equipped with an Agilent Plgel 5 μm Guard Column (50 x 7,5 mm) used as precolumn. The molecular weights of the polyesters were determined from the calibration curve (covering a molecular weight ranging from 532 to 2400000 g/mol), obtained using the Agilent ReadyCal-Kit PSS GPC/SEC Polymer Standards and fitted with a fifth-order polynomial regression curve.

3. Results and discussion

3.1. Enzyme immobilization on polypropylene beads

LCC, LCC^{ICCG} and Thb were immobilized onto Accurell MP 1000 (polypropylene) beads by employing a biocatalyst loading of 1 % w/w relative to the amount of solid support. To assess the efficiency of the immobilization procedure, the protein content and esterase activity were measured in the supernatant collected at defined time-points (0, 1, 2, 4, 8, 24 h) via Bradford Assay and the *p*-NPB based Esterase Activity Assay, respectively. These measurements allowed to monitor the progressive reduction of enzyme in solutions, thereby confirming its successful adsorption onto the support. As shown in Fig. 1a, the enzyme activity declined over time, corresponding to the decrease of free enzyme in the supernatant. Protein quantification results were also expressed as residual protein concentration (%) for the same time-points (Fig. 1b). After 24 h of immobilization, the enzymatic activity in the supernatant was below 2 % for LCC and below 1 % for LCC^{ICCG} with both enzymes exhibiting residual concentration below 7 %, indicating an effective immobilization. Notably, within just 2 h of immobilization, both residual activity and protein concentration for the two enzymes have dropped below 22 % pointing out a very similar adsorption pattern onto the support. The decrease in concentration and catalytic activity in the supernatant corresponds to increased activity of the immobilized fraction on polypropylene beads. To demonstrate this, a qualitative Esterase Activity Assay was performed using *p*-NPB as a model substrate, which allowed visual detection of enzymatic activity via the release of yellow-colored *para*-nitrophenol upon hydrolysis. As visible from Fig. S3, this colorimetric assay clearly confirmed that the immobilized enzymes (LCC, LCC^{ICCG} and Thb) retained catalytic activity, in contrast to control samples with only unmodified polypropylene beads, where no color change was observed, providing visual evidence of retained enzymatic activity post-immobilization.

The comparable adsorption profile of LCC and LCC^{ICCG} was expected since structural integrity was preserved through rational site-directed mutagenesis: the introduced mutation did not alter the catalytic triad of the active site (Ser_{165}, Asp_{210} and His_{242}) as well as the hydrophobic to hydrophilic ratio on the enzyme's surface (Fig. S4). Briefly, as well documented in the literature(Sowdhamini et al., 1989), in the LCC enzyme structure, the interatomic distances between the Cα atoms (4.5 Å) and Cβ atoms (4.4 Å) of residues Asp_{238} and Ser_{283} were within the range suitable for introducing a disulfide bridge (represented by spheres in Fig. S4). A variant containing the D238C and S283C mutations was created, resulting in a disulfide-bond that enhanced the enzyme's thermal stability, although with reduced activity. To counteract this reduction, the F243I mutation was introduced, yielding the F243I/D238C/S283C (ICC) variant, which showed improved specific activity. Finally, the Y127G mutation was added to further improve thermostability, leading to the development of the quadruple mutant F243I/D238C/S283C/Y127G (ICCG)(Tournier et al., 2020). Furthermore, a similar adsorption behavior was observed also in the case of Thb enzyme, where less than 1 % of both residual activity and protein concentration remained in the supernatant after 24 h, indicating that almost all the biocatalyst was effectively adsorbed onto the solid support. In light of these comparable absorption profiles, it was hypothesized that enzyme immobilization efficiency on the hydrophobic polypropylene beads could be influenced by the surface hydrophobicity of the enzyme. To explore this, the composition of surface-exposed amino acids for each enzyme was evaluated by calculating their superficial hydrophobic to hydrophilic ratio (Fig. S5). As anticipated above, LCC and its variant LCC^{ICCG} exhibited an identical surface hydrophobicity of 34 %; likewise, Thb showed a comparable value of 35 %. These findings suggested that the similar immobilization behavior of the three enzymes could be ascribed to their nearly identical surface hydrophobicity.

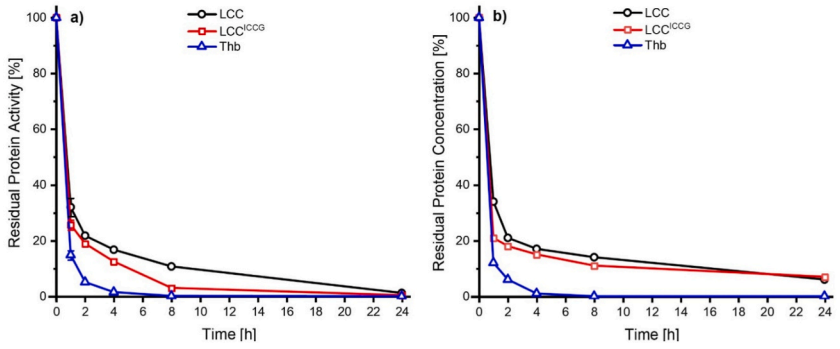

Fig. 1. Immobilization of hydrolases LCC, LCC^{ICCCG} and Thb on polypropylene beads. Graphical illustration of residual protein activity (a) and residual protein concentration (b) of the different timepoint supernatants for LCC (black circles), LCC^{ICCG} (red squares) and Thb (blue triangles) respectively. All the measurements for the three enzymes were performed in triplicates with standard deviation (σ) < 0,05 in graph a while <0,4 in graph b with the exception of t = 1.

3.2. Design of experiment (DoE) assisted study

The potential of LCC, LCC^{ICCG} and Thb in synthetic reactions has not been assessed previously, despite their noted effectiveness in polyester degradation. Therefore, a full factorial experimental design was developed using MODDE® Pro 13 Software to study the thermostability and substrate selectivity of the three enzymes in short-esters synthesis reactions using alcohols and diacids with varying chain length (alcohol chain length = C4, C8, and C12; acid chain length = C4, C8 and C12).

As discussed in section 2.7, the DoE was employed to systematically investigate the overall influence of four selected independent variables (temperature, alcohol chain length, acid chain length and reaction time) on the resulting outcome, with acid conversion rate (measured via GC analysis) serving as response variable for each experimental condition. Moreover, the list of reactions carried out for each enzyme as part of the DoE is reported in Table S1, while Fig. 2 provides a schematic overview of short-ester synthesis reaction. Upon completion of each DoE reaction, the results of the experiments were graphically evaluated using a 4D contour plot, provided by the software for each enzyme. Model coefficients are plotted along the axes with temperature on the horizontal-axis and acid chain length on the vertical-axis, while the reaction times and the alcohol chain lengths are held constant for each of the nine final profiles that constitute the 4D contour response. The efficiency of the reaction in terms of acid conversion [%] is represented by a color-coded gradient, ranging from blue for lower conversions to red for the highest.

3.2.1. LCC-catalyzed esterification reaction: 4D contour response analysis

The LCC 4D Contour Response showed that, as expected, the conversion continued to increase within the time frame explored (6 h), indicating that the enzyme preserved its activity even at high temperatures. As visible from Fig. 3, similarly to previously reported trends for CaLB and HiC(Fabbri et al., 2021), LCC revealed a clear preference for long-chain alcohols and acids under identical experimental conditions, despite exhibiting comparatively lower conversion rates (~40 % efficiency reduction with respect to the commercial hydrolytic enzymes CaLB and HiC where >90 % of monomers conversion were reported(Fabbri et al., 2021). Specifically, when C12 alcohol was used, conversion rates over 55 % were achieved after 6 h. On the other hand, aligning with the previously reported CaLB and HiC selectivity pattern(Fabbri et al., 2021), when reacting with short-chain alcohols and acids (C4 or C6 chain length), the enzyme showed lower conversion rates (below 30 %) even after 6 h of reaction with ~50 % efficiency reduction with respect to long-chain alcohol and acids. This behaviour contrasts with that of Thc_Cut1, which exhibited a substrate specificity favouring short-chain alcohols (C4) and medium-chain acids (C8) although showing low overall conversion rates(Fabbri et al., 2021), thereby underscoring the different selectivity between these enzymes. Moreover, Fig. S6 provides additional evidence for LCC's selectivity towards long-chain alcohols and acids demonstrating that the highest efficiency (~69 % of conversion rate) was reached using C12 alcohol (1-dodecanol) combined with C12 acid (lauric acid). Furthermore, LCC exhibited its optimal catalytic activity within the 50–60 °C range, with a significant reduction in conversion efficiency observed at temperatures above 75 °C. To more precisely define LCC optimal temperature (T_{opt}), additional reactions using the most efficient substrate combination (alcohol = 12 with acid = 12) were carried out at selected temperatures in the 50–70 °C range (specifically 55 °C, 60 °C and 65 °C). The highest conversion (~78 %) was observed at 60 °C, as reported in Fig. S7, corresponding to the T_{opt} of the enzyme.

3.2.2. LCC^{ICCG}-catalyzed esterification reaction: 4D contour response analysis

The 4D contour response derived from the DoE using LCC^{ICCG} revealed a pattern similar to that observed for LCC. As illustrated in Fig. 4, LCC^{ICCG} exhibited a clear preference for long-chain alcohols and acids. Notably, a conversion rate exceeding 55 % was achieved after 6 h of reaction when using the 12 carbon-chain alcohol. In the case of C8 acid, a ~35 % efficiency reduction moving from lower to higher temperature was observed. Conversely, as visible in the upper-left panel of Fig. 4, LCC^{ICCG} showed limited conversion rates (below 15 %) when processing short-chain alcohols and acids (4 and 6 carbon chain length) even after 6h of reaction, with ~75 % efficiency reduction than long-chain alcohol and acids. Furthermore, Fig. S8 demonstrates LCC^{ICCG}'s preference for long-chain alcohols and medium/long-chain acids. Interestingly, although LCC and LCC^{ICCG} exhibited a similar trend with comparable conversion efficiency for this class of substrates, the mutant variant achieved the higher conversion rate (~68 %) when using 1-dodecanol (C12 alcohol) and octanoic acid (C8 acid). In terms of thermostability, LCC^{ICCG} showed optimal catalytic activity in the 50–60 °C temperature range. A noticeable reduction in conversion efficiency occurred above 75 °C, in agreement with results obtained for LCC. To accurately determine the T_{opt} of LCC^{ICCG}, a series of reactions were conducted using the most effective substrate combination (alcohol = 12 with acid = 8) focusing on selected temperatures in the 50–70 °C range (specifically 55 °C, 60 °C and 65 °C). As visible from Fig. S9 maximum conversion rate (~74 %) was achieved at 55 °C, defining it as LCC^{ICCG} T_{opt}. Notably, LCC^{ICCG} exhibits enhanced

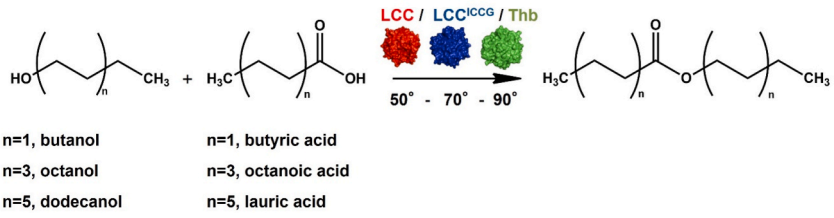

Fig. 2. Schematic overview of short-ester synthesis reaction: LCC/LCC^{ICCG}/Thb-catalyzed synthesis using C4, C8, and C12 alcohol and acid to obtain C8, C12, C16, C20 and C24 esters.

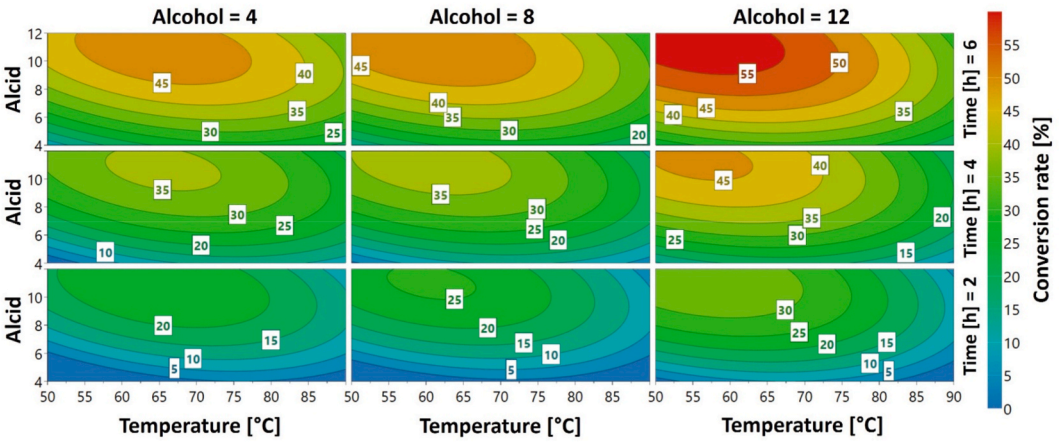

Fig. 3. Synthesis of C8, C12, C16, C20 and C24 esters from alcohols and acids of varying chain length: LCC 4D contour response. Every graph illustrates a specific alcohol chain length (with 4,8 and 12 carbon atoms) at a distinct reaction time (2, 4 and 6 h). The Y-axis corresponds to acid chain length (varying from C4 to C12) while the X-axis represents the Temperature [°C]. Conversion rates (values in the white square) are indicated using different colors, as indicated in the legend on the right.

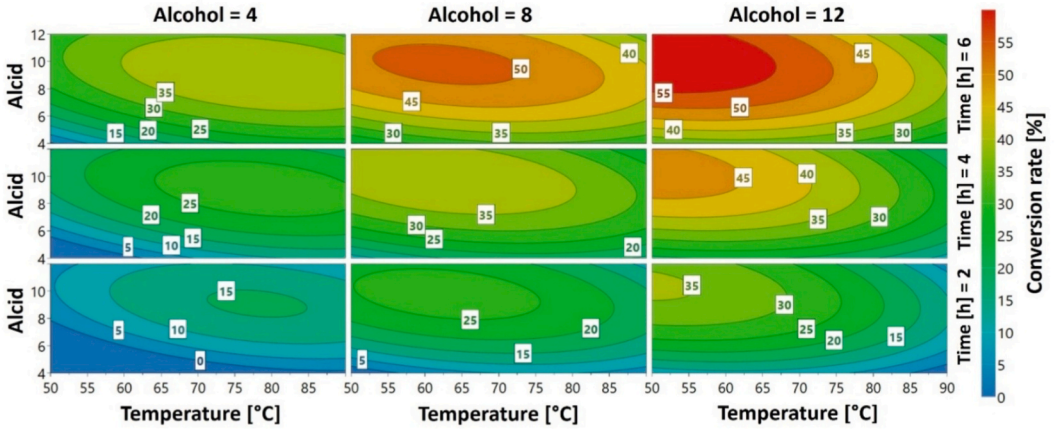

Fig. 4. Synthesis of C8, C12, C16, C20 and C24 esters from alcohols and acids of varying chain length: LCC^{ICCG} 4D contour response. Every graph illustrates a specific alcohol chain length (with 4,8 and 12 carbon atoms) at a distinct reaction time (2, 4 and 6 h). The Y-axis corresponds to acid chain length (varying from C4 to C12) while the X-axis represents the Temperature [°C]. Conversion rates (values in the white square) are indicated using different colors, as indicated in the legend on the right.

thermostability for PET degradation, functioning efficiently at elevated temperatures(Kumar et al., 2025). However, during synthetic reactions performed in this study, its optimal activity shifted to lower temperatures. This difference reflects the distinct stability and activity requirements between hydrolytic and synthetic conditions. These results on thermal stability and substrate selectivity suggest that the engineered mutations may contribute to slight alterations in enzymatic behavior between the LCC and LCC^{ICCG} variants. While the catalytic triad of the active site (Ser_{165}, Asp_{210} and His_{242}) is conserved, the introduced D238C and S283C mutations, associated with the formation of a disulfide-bond as mentioned above in section 3.1, as well as F243I mutation are situated in close proximity to the active site (Fig. S10). It is hypothesized that these structural alterations are likely to induce conformational rearrangements around the active site, thereby potentially affecting both substrate selectivity and thermostability, not only in depolymerization reactions but also in esterification synthesis.

3.2.3. Thb-catalyzed esterification reaction: 4D contour response analysis

Also, in the case of Thb, the conversion rate continued rising across the 6-h reaction period, indicating sustained enzymatic activity over time at high temperature. However, as visible from Fig. 5, the resulting conversions were significantly lower compared to those achieved with LCC and LCC^{ICCG}. The highest conversion was above 11 % after 6 h, although no clear preference towards a specific substrate was observed. Fig. S11 further supports the absence of substrate selectivity, as reflected by the consistently similar conversion values across the tested substrate combinations. Specifically, Thb achieved nearly identical conversions when combining C12 alcohol with either C8 or C12 acid (~18 %), C8 alcohol with the same acids (~16 %), and even C4 alcohol with C8 or C12 acids (~15

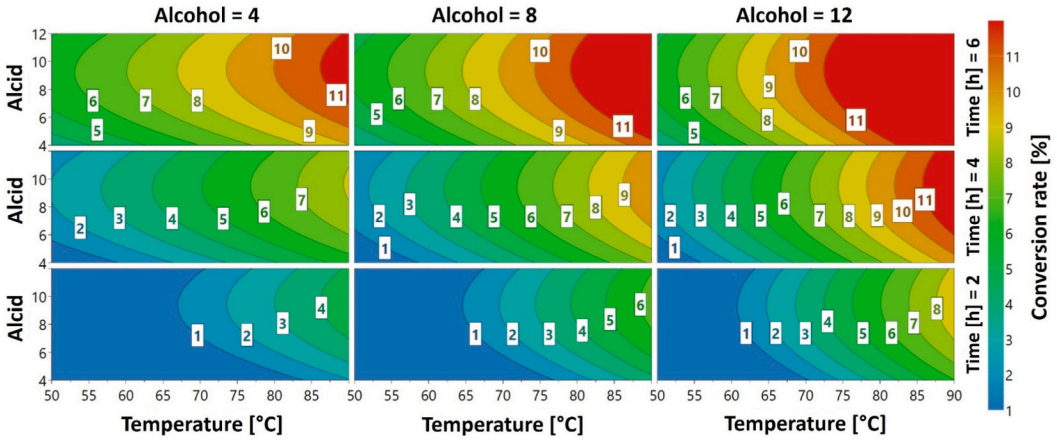

Fig. 5. Synthesis of C8, C12, C16, C20 and C24 esters from alcohols and acids of varying chain length: Thb 4D contour response. Every graph illustrates a specific alcohol chain length (with 4,8 and 12 carbon atoms) at a distinct reaction time (2, 4 and 6 h). The Y-axis corresponds to acid chain length (varying from C4 to C12) while the X-axis represents the Temperature [°C]. Conversion rates (values in the white square) are indicated using different colors, as indicated in the legend on the right.

%). In the case of short-chain acid (C4), conversion varied between 5 % and 11 % (up to ~12 % processing C12 alcohol with C4 acid), with higher efficiency observed at higher temperature. Unlike LCC and LCC^{ICCG}, it was not meaningful to determine precisely at which temperature Thb exhibited its optimal activity, due to the minimal variation in conversion efficiency across all the tested temperatures (just ~6 % of variation in the entire 50–90 °C range). However, the maximum conversions were reached in the temperature range between 75 and 90 °C. Although Thb showed limited efficiency in short-esters synthesis, this high thermal stability makes it a promising candidate for further synthetic applications, particularly in polycondensation reaction where the T_{opt} will be accurately investigated.

3.3. *LCC/LCC^{ICCG}/Thb-catalyzed polycondensation reactions*

Short-esters synthesis reactions were conducted to define the optimal synthetic conditions of the three enzymes. To assess the applicability of the developed 4D contour models also in the production of larger macromolecules, the three hydrolases were also compared in polycondensation reactions. In particular, to evaluate the potential of alternative biocatalysts to CaLB in synthetic applications, the new enzymes were analyzed using the monomer combination of dimethyl adipate (DMA) and 1,8-octanediol (ODO), previously identified as the most effective for CaLB-catalyzed polycondensation(Pellis et al., 2018). Based on this, enzyme catalyzed reactions were conducted at the corresponding T_{opt} of LCC (60 °C) and LCC^{ICCG} (55 °C) using DMA and ODO as biobased precursors for polyester synthesis (Fig. S12),while the T_{opt} of Thb was precisely determined by performing the same reaction in the 75–90 °C range. Consistent to what discussed in section 2.7, the catalytic mechanism in polyester synthesis proceeds through two steps(Loos, 2022). In the specific case of a model transesterification between dimethyl adipate and 1,8-octanediol, the first step involves the acylation of Ser_{165} (for the two LCC variants) and Ser_{131} (for Thb) by the diester, proceeding through a tetrahedral intermediate. The second step consist of a deacylation step of Ser_{165} (for the two LCC variants) and Ser_{131} (for Thb) by nucleophilic attack of the diol, regenerating the free Ser and making it available for the next cycle of chain elongation.

The progress of the reaction was monitored by using ^{1}H NMR spectroscopy and Gel Permeation Chromatography (GPC). For all the three enzymes, analysis of the ^{1}H NMR spectra revealed a similar extent of monomer conversion. As visible from Fig. 6a, this was evidenced by the intensity reduction in the signal at 3.6 ppm, corresponding to the disappearance of both the $–CH_2$-CH_2-OH group from the diol and of the $–OCH_3$ group from the diester, ascribed to the release of MeOH as by-product. Concurrently, an intensity increase in the signal at 4.1 ppm was observed as clear indication of the formation of $–CH_2$-CH_2-*O*-C═O ester bond. This outcome was not observed in the control experiment, where the polycondensation reaction was carried out using unmodified polypropylene beads. As visible in Fig. 6a, no signal reduction was observed at 3.6 ppm, indicating that the $–OCH_3$ persists and the $–CH_2$-*O*-C═O moiety is not formed as a confirmation of the unsuccessful synthesis of the target polyester, with monomer conversion limited to only 4 %.

In contrast, as expected, comparable monomer conversion rates (~91 %), M_n (~3600 Da) and degree of polymerization (~ 14) were achieved using LCC and LCC^{ICCG} respectively, as shown in Fig. 6b and Table S2. These results demonstrated the high catalytic activity towards long-chain diols, confirming the trend seen for the synthesis of short-esters (Section 3.2.1 and Section 3.2.2). When compared to literature reports on enzymatic polymerization of DMA and ODO catalyzed by CaLB and HiC immobilized on polypropylene beads at their corresponding T_{opt} (85 °C for CaLB and 70 °C for HiC)(Fabbri et al., 2021), LCC and LCC^{ICCG} exhibited comparable monomer conversion rates (~6 % lower than CaLB and ~5 % higher than HiC). Conversely, GPC analysis revealed a M_n of approximately 3600 Da for both LCC and its variant form, which is significantly lower than the 8100 Da achieved using CaLB (~57 % M_n reduction), but notably higher than the 1400 Da reported for HiC (~60 % M_n increase).

In a next step, enzymatic polycondensation of DMA and ODO was performed using Thb to assess precisely its T_{opt}. The same

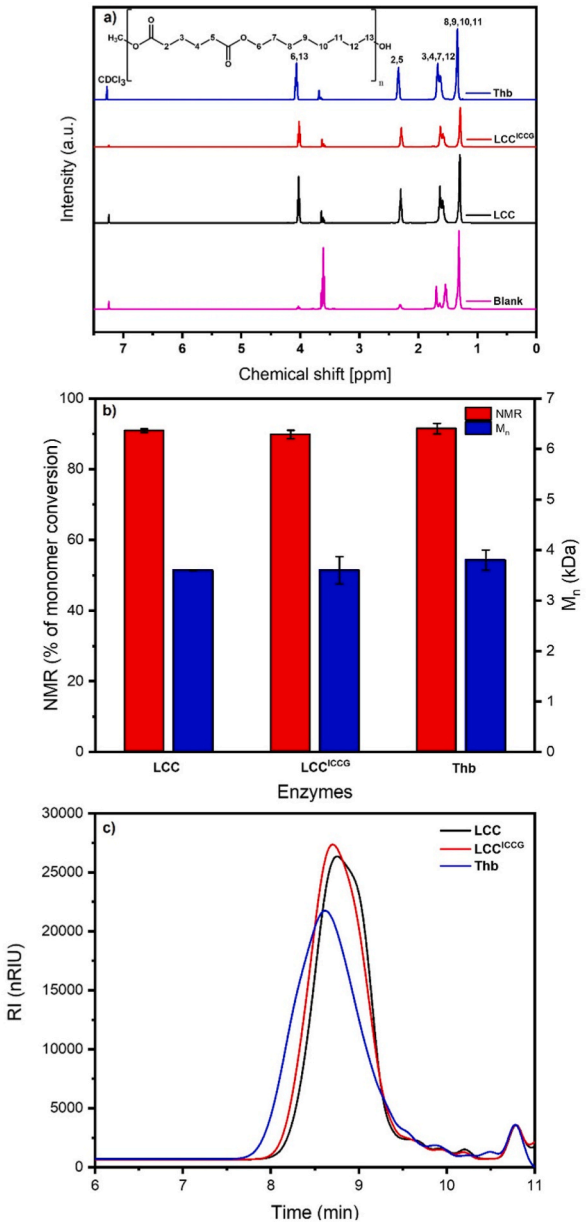

Fig. 6. a) Comparison of ^{1}H NMR spectra of poly(1,8-octylene adipate) synthesized using the three enzymes: LCC (black), LCC^{ICCG} (red) and Thb (blue), alongside control experiment (magenta) performed with polypropylene beads in the absence of enzyme; b) Progression of reactions monitored via ^{1}H NMR (% of monomer conversion, red bars) and GPC (number average molecular weight, blue bars) for the three enzymes. All the measurements for the three enzymes were performed in triplicates: the figure shows the mean with standard deviation (σ) < 1,5 % of monomer conversion rate while <0,3 Da for M_n; (c) GPC charts of the polymer length distribution for polycondensation reaction catalyzed by LCC (black), LCC^{ICCG} (red) and Thb (blue).

reaction was carried out focusing on selected temperatures between 75 and 90 °C (specifically 75 °C, 80 °C, 85 °C and 90 °C), predicted as the optimal range from the previously proven model on short-esters synthesis reactions (Section 3.3). As visible from Fig. S13, the T_{opt} turned out to be at 80 °C, where both monomer conversion rate and M_n were higher than the other temperatures (92 % and M_n of 3800 Da) in which Thb exhibited a reduced activity (54 %, 62 % and 23 % of conversion rate while 1250, 1060 and 840 Da at 75 °C, 85 °C and 90 °C respectively). Unexpectedly, ^{1}H NMR and GPC analysis (Fig. 6a and b) revealed that the highest conversion rate of approximately 92 % and with a M_n of 3800 Da was achieved at 80 °C, comparable to the values seen for the two LCC variants at a temperature of 60 and 55 °C. GPC charts of polycondensation progress for each of the three enzymes is reported in Fig. 6c.

Therefore, contrary to the poor efficiency in short-esters synthesis, Thb has been demonstrated to preferentially catalyze reactions involving long-chain diols and diesters in synthetic applications. To the best of our knowledge, such behavior has not been documented

yet and is in contrast with previously published data reporting higher enzymatic efficiency in short-esters synthesis(Fabbri et al., 2024).

4. Conclusions

In summary, LCC, LCC^{ICCG} and Thb were effectively immobilized onto polypropylene beads. A full factorial design of experiments (DoE) was used to determine their optimal synthetic conditions. Both LCC and LCC^{ICCG} demonstrate a clear preference for long-chain alcohols and medium/long chain acids with T_{opt} of 60 °C and 55 °C, respectively. On the other hand, Thb exhibits its highest catalytic activity efficiency in polycondensation reaction at 80 °C, confirming its thermophilic nature, despite low esterification performance in short-esters synthesis reaction. To investigate their applicability in the synthesis of higher molecular weight polyesters, the T_{opt} of the three enzymes was tested in polycondensation reactions using dimethyl adipate and 1,8-octanediol as biobased building blocks. The three enzymes catalyzed formation of polyesters with comparable monomer conversion rates and M_n values (91 % and 3600 Da for LCC and LCC^{ICCG} *vs* 92 % and 3800 Da for Thb). In conclusion, these results underscore the promising capabilities of these thermophilic enzymes in polyester synthesis, expanding the application of PET hydrolases from depolymerization to synthetic processes. Although exhibiting an approximate 57 % reduction in M_n when compared to CaLB, their overall catalytic performance, especially in comparison to HiC and Thc_Cut1, demonstrates their value as viable alternatives for sustainable biocatalyzed synthesis of polyesters.

CRediT authorship contribution statement

Francesco Papatola: Writing – review & editing, Writing – original draft, Software, Methodology, Investigation, Formal analysis, Data curation. **Filippo Fabbri:** Writing – review & editing, Validation, Supervision, Methodology, Investigation. **Virender Kumar:** Writing – review & editing, Validation, Methodology, Investigation. **Chiara Siracusa:** Writing – review & editing, Methodology, Investigation. **Felice Quartinello:** Writing – review & editing, Visualization, Validation, Data curation. **Doris Ribitsch:** Writing – review & editing, Visualization, Validation, Supervision. **Cristiano Varrone:** Writing – review & editing, Visualization, Validation, Supervision, Resources, Project administration, Conceptualization. **Georg M. Guebitz:** Writing – review & editing, Visualization, Validation, Resources, Project administration. **Alessandro Pellis:** Writing – review & editing, Visualization, Validation, Supervision, Resources, Project administration, Conceptualization.

Declaration of competing interest

The authors declare that they have no known competing financial interests or personal relationships that could have appeared to influence the work reported in this paper.

Acknowledgments

Funded by the European Union (ERC, CIRCULARIZE, 101114664) and H2020 UPLIFT project (Grant agreement no. 953073). Views and opinions expressed are, however, those of the author(s) only and do not necessarily reflect those of the European Union or the European Research Council. Neither the European Union nor the granting authority can be held responsible for them.

Appendix A. Supplementary data

Supplementary data to this article can be found online at https://doi.org/10.1016/j.scp.2025.102260.

Data availability

Data will be made available on request.

References

Arnal, G., Anglade, J., Gavalda, S., Tournier, V., Chabot, N., Bornscheuer, U.T., Weber, G., Marty, A., 2023. Assessment of four engineered PET degrading enzymes considering large-scale industrial applications. ACS Catal. 13, 13156–13166. https://doi.org/10.1021/acscatal.3c02922.

Fabbri, F., Bertolini, F.A., Guebitz, G.M., Pellis, A., 2021. Biocatalyzed synthesis of flavor esters and polyesters: a design of experiments (DoE) approach. Int. J. Mol. Sci. 22, 8493. https://doi.org/10.3390/ijms22168493.

Fabbri, F., Vergani, I., Donoso, S., Nespoli, L., Rocca, V.M., Moni, L., Guebitz, G.M., Contente, M.L., Pellis, A., 2024. Mycobacterium smegmatis acyltransferase catalyzes the synthesis of esters and polyesters. RSC Sustain. 2, 1372–1377. https://doi.org/10.1039/D4SU00038B.

Feder, D., Gross, R.A., 2010. Exploring chain length selectivity in HIC-catalyzed polycondensation reactions. Biomacromolecules 11, 690–697. https://doi.org/10.1021/bm901272r.

Guarneri, A., Cutifani, V., Cespugli, M., Pellis, A., Vassallo, R., Asaro, F., Ebert, C., Gardossi, L., 2019. Functionalization of enzymatically synthesized rigid poly (itaconate) s via post-polymerization Aza-Michael addition of primary amines. Adv. Synth. Catal. 361, 2559–2573. https://doi.org/10.1002/adsc.201900055.

Han, X., Liu, W., Huang, J.-W., Ma, J., Zheng, Y., Ko, T.-P., Xu, L., Cheng, Y.-S., Chen, C.-C., Guo, R.-T., 2017. Structural insight into catalytic mechanism of PET hydrolase. Nat. Commun. 8, 2106. https://doi.org/10.1038/s41467-017-02255-z.

Hanefeld, U., Gardossi, L., Magner, E., 2009. Understanding enzyme immobilisation. Chem. Soc. Rev. 38, 453–468. https://doi.org/10.1039/b711564b.
Hunsen, M., Azim, A., Mang, H., Wallner, S.R., Ronkvist, A., Wenchun, X., Gross, R.A., 2007. A cutinase with polyester synthesis activity. Macromolecules 40, 148–150. https://doi.org/10.1021/ma062095g.
Illanes, A., Cauerhff, A., Wilson, L., Castro, G.R., 2012. Recent trends in biocatalysis engineering. Bioresour. Technol. 115, 48–57. https://doi.org/10.1016/j.biortech.2011.12.050.
Kobayashi, S., 2010. Lipase-catalyzed polyester synthesis - a green polymer chemistry. Proc. Japan Acad. Ser. B Phys. Biol. Sci. https://doi.org/10.2183/pjab.86.338.
Kobayashi, S., Makino, A., 2009. Enzymatic polymer synthesis: an opportunity for green polymer chemistry. Chem. Rev. 109, 5288–5353. https://doi.org/10.1021/cr900165z.
Kumar, V., Pellis, A., Wimmer, R., Popok, V., Christiansen, J. de C., Varrone, C., 2024. Efficient depolymerization of Poly(ethylene 2,5-furanoate) using polyester hydrolases. ACS Sustain. Chem. Eng. 12, 9658–9668. https://doi.org/10.1021/acssuschemeng.4c00915.
Kumar, V., Wimmer, R., Varrone, C., 2025. Efficient bioprocess for mixed PET waste depolymerization using crude cutinase. Polymers 17, 763. https://doi.org/10.3390/polym17060763.
Li, Qiang, Liu, W., Jing, N., Li, Qingqing, Yang, K., Wang, X., Yao, J., 2023. Attack site density of a highly-efficient PET hydrolases. Protein pept. Lett 30, 506–512. https://doi.org/10.2174/0929866530666230509141807.
Loos, K., 2022. Biocatalysis in Polymer Chemistry. Wiley Online Library. https://doi.org/10.1002/9783527632534.
Mahapatro, A., Kalra, B., Kumar, A., Gross, R.A., 2003. Lipase-catalyzed polycondensations: effect of substrates and solvent on chain formation, dispersity, and end-group structure. Biomacromolecules 4, 544–551. https://doi.org/10.1021/bm0257208.
Pellis, A., Comerford, J.W., Maneffa, A.J., Sipponen, M.H., Clark, J.H., Farmer, T.J., 2018. Elucidating enzymatic polymerisations: Chain-length selectivity of Candida Antarctica lipase B towards various aliphatic diols and dicarboxylic acid diesters. Eur. Polym. J. 106, 79–84. https://doi.org/10.1016/j.eurpolymj.2018.07.009.
Pellis, A., Corici, L., Sinigoi, L., D'Amelio, N., Fattor, D., Ferrario, V., Ebert, C., Gardossi, L., 2015. Towards feasible and scalable solvent-free enzymatic polycondensations: integrating robust biocatalysts with thin film reactions. Green Chem. 17, 1756–1766. https://doi.org/10.1039/c4gc02289k.
Pellis, A., Ferrario, V., Cespugli, M., Corici, L., Guarneri, A., Zartl, B., Acero, E.H., Ebert, C., Guebitz, G.M., Gardossi, L., 2017a. Fully renewable polyesters: via polycondensation catalyzed by Thermobifida cellulosilytica cutinase 1: an integrated approach. Green Chem. 19, 490–502. https://doi.org/10.1039/c6gc02142e.
Pellis, A., Ferrario, V., Zartl, B., Brandauer, M., Gamerith, C., Acero, E.H., Ebert, C., Gardossi, L., Guebitz, G.M., 2016a. Enlarging the tools for efficient enzymatic polycondensation: structural and catalytic features of cutinase 1 from Thermobifida cellulosilytica. Catal. Sci. Technol. 6, 3430–3442. https://doi.org/10.1039/C5CY01746G.
Pellis, A., Herrero Acero, E., Gardossi, L., Ferrario, V., Guebitz, G.M., 2016b. Renewable building blocks for sustainable polyesters: new biotechnological routes for greener plastics. Polym. Int. https://doi.org/10.1002/pi.5087.
Pellis, A., Vastano, M., Quartinello, F., Herrero Acero, E., Guebitz, G.M., 2017b. His-tag immobilization of cutinase 1 from Thermobifida cellulosilytica for solvent-free synthesis of polyesters. Biotechnol. J. 12, 1700322. https://doi.org/10.1002/biot.201700322.
Ran, N., Zhao, L., Chen, Z., Tao, J., 2008. Recent applications of biocatalysis in developing green chemistry for chemical synthesis at the industrial scale. Green Chem. 10, 361–372. https://doi.org/10.1039/B716045C.
Richter, P.K., Blázquez-Sánchez, P., Zhao, Z., Engelberger, F., Wiebeler, C., Künze, G., Frank, R., Krinke, D., Frezzotti, E., Lihanova, Y., Falkenstein, P., Matysik, J., Zimmermann, W., Sträter, N., Sonnendecker, C., 2023. Structure and function of the metagenomic plastic-degrading polyester hydrolase PHL7 bound to its product. Nat. Commun. 14, 1905. https://doi.org/10.1038/s41467-023-37415-x.
Sheldon, R.A., 2007. Enzyme immobilization: the quest for optimum performance. Adv. Synth. Catal. 349, 1289–1307. https://doi.org/10.1002/adsc.200700082.
Sheldon, R.A., van Pelt, S., 2013. Enzyme immobilisation in biocatalysis: why, what and how. Chem. Soc. Rev. 42, 6223–6235. https://doi.org/10.1039/C3CS60075K.
Siracusa, C., Fohler, L., Leibetseder, L., Striedner, G., Oostenbrink, C., Quartinello, F., Guebitz, G.M., Ribitsch, D., 2025. Activity of an anaerobic Thermoanaerobacterales hydrolase on aliphatic and aromatic polyesters. Front. Bioeng. Biotechnol. 12, 1520680. https://doi.org/10.3389/fbioe.2024.1520680.
Sonnendecker, C., Oeser, J., Richter, P.K., Hille, P., Zhao, Z., Fischer, C., Lippold, H., Blázquez-Sánchez, P., Engelberger, F., Ramírez-Sarmiento, C.A., Oeser, T., Lihanova, Y., Frank, R., Jahnke, H.G., Billig, S., Abel, B., Sträter, N., Matysik, J., Zimmermann, W., 2022. Low carbon footprint recycling of post-consumer PET plastic with a metagenomic polyester hydrolase. ChemSusChem 15, e202101062. https://doi.org/10.1002/cssc.202101062.
Sowdhamini, R., Srinivasan, N., Shoichet, B., Santi, D.V., Ramakrishnan, C., Balaram, P., 1989. Stereochemical modeling of disulfide bridges. Criteria for introduction into proteins by site-directed mutagenesis. Protein Eng. Des. Sel. 3, 95–103. https://doi.org/10.1093/protein/3.2.95.
Sulaiman, S., Yamato, S., Kanaya, E., Kim, J.J., Koga, Y., Takano, K., Kanaya, S., 2012. Isolation of a novel cutinase homolog with polyethylene terephthalate-degrading activity from leaf-branch compost by using a metagenomic approach. Appl. Environ. Microbiol. 78, 1556–1562. https://doi.org/10.1128/AEM.06725-11.
Tao, J., Kazlauskas, R., 2011. Biocatalysis for Green Chemistry and Chemical Process Development. Wiley Online Library. https://doi.org/10.1002/9781118028308.
Tournier, V., Topham, C.M., Gilles, A., David, B., Folgoas, C., Moya-Leclair, E., Kamionka, E., Desrousseaux, M.L., Texier, H., Gavalda, S., Cot, M., Guémard, E., Dalibey, M., Nomme, J., Cioci, G., Barbe, S., Chateau, M., André, I., Duquesne, S., Marty, A., 2020. An engineered PET depolymerase to break down and recycle plastic bottles. Nature 580, 216–219. https://doi.org/10.1038/s41586-020-2149-4.
Williams, C.K., 2007. Synthesis of functionalized biodegradable polyesters. Chem. Soc. Rev. 36, 1573–1580. https://doi.org/10.1039/B614342N.